

# Experimental studies on rectangular jets with trapezoidal tabs

**A. Arokkiaswamy**

argy\_swamy@hotmail.com

**S. B. Verma**

sbverma@ead.cmmacs.ernet.in

**S. Venkateswaran**

venkatesh\_w@hotmail.com

Council of Scientific and Industrial Research  
National Aerospace Laboratory  
Bangalore, India

## ABSTRACT

An experimental investigation was carried out to study the flow development of a jet issuing from a 2:1 rectangular nozzle with mixing tabs using two-component hotwire anemometry. A pair of tabs of trapezoidal configuration (with 2% total blockage area) is placed on the minor-axis side of the rectangular nozzle and tested for two tab inclination angles of 135° and 45°, with respect to the flow direction. Tests were conducted for a nominal jet exit velocity of 20m/sec corresponding to a Reynolds number based on nozzle equivalent diameter of  $5.013 \times 10^4$ . Relative to the plain jet, the jet with tabs show significant reduction in jet-core length (by 67%) followed by a faster decay in jet centreline velocity ( $U/U_e$ ). This is also accompanied by a significant upstream shift in peak centreline turbulence intensity ( $u'/U_e$ ). The presence of tabs is observed to inhibit the jet growth along the minor-axis plane thereby introducing large distortion in the jet cross-sectional development that ultimately leads to jet-core bifurcation along its major-axis. While a mushroom-like flow structure develops behind the tab with 135° inclination, the flow structure behind a 45° inclined tab rather takes the shape of the tab itself. The former flow development is seen to enhance the jet growth more along the minor-axis while the latter improves the jet growth more along the major-axis plane. From application point of view, since both tab inclinations result in more or less similar jet characteristics, a 135° inclined tab would be preferable over a 45° inclined tab from the view of improved jet mixing.

## NOMENCLATURE

|               |  |
|---------------|--|
| $D_e$         | equivalent diameter of the rectangular nozzle, mm                      |
| $h$           | projected height of the tab to the oncoming flow, mm                   |
| $Re_{De}$     | Reynolds number based on equivalent diameter of the rectangular nozzle |
| $u'/U_e$      | non-dimensional streamwise velocity fluctuation                        |
| $u'v'/U_e^2$  | Reynolds shear stress  |
| $U_e$         | mean streamwise jet exit velocity, $\text{ms}^{-1}$                    |
| $U$           | local mean streamwise jet velocity, $\text{ms}^{-1}$                   |
| $V$           | local mean jet velocity along $Y$ -direction, $\text{ms}^{-1}$         |
| $X$           | streamwise distance along the jet centreline, mm                       |
| $Y$           | cross-stream distance along minor-axis plane, mm                       |
| $Z$           | cross-stream distance along major-axis plane, mm                       |
| $Y_{0.5}$     | jet half-width growth along minor-axis plane, mm                       |
| $Z_{0.5}$     | jet half-width growth along major-axis plane, mm                       |
| $w$           | width of the tab base, mm  |
| $\delta_{mi}$ | jet exit shear-layer thickness along minor-axis plane, mm              |
| $\delta_{mj}$ | jet exit shear-layer thickness along major-axis plane, mm              |
| $\phi$        | tab angle relative to the flow direction, degrees                      |

## 1.0 INTRODUCTION

Mixing enhancement in jet flows is of paramount importance in many engineering applications and therefore, has been the subject of continuing research. Frequently the jet geometry is dictated by the nature of application since jet characteristics are known to be closely related to the dynamics of shear flow originating at the nozzle exit and hence, are strongly affected by the shape of the nozzle from which they issue<sup>(1)</sup>. As a result one of the most commonly used methods of shear flow control in jets is the use of nozzles with non-circular exit cross-sections which significantly changes the jet flow development as compared to a jet issuing from a circular nozzle. Jets from non-circular nozzle geometries spread and mix faster thereby providing a unique capability to control the jet development (both fine- and large-scale).

Studies on jets issuing from non-circular nozzle geometries such as triangular<sup>(2)</sup>, square<sup>(3)</sup>, rectangular<sup>(4,5)</sup> and elliptic<sup>(6-9)</sup> have been reported in the past. It has been found that the initial instability mode in a jet issuing from an elliptic nozzle is strongly linked to the thinnest jet momentum thickness around the nozzle circumference<sup>(6,10)</sup>. Rectangular jets<sup>(11)</sup>, on the other hand, combine the aspect ratio features of an elliptic jet with the corner (vertex) features of square jets. Later studies<sup>(4,7)</sup> on the coherent structures of non-circular jets revealed that the jet undergoes a three-dimensional deformation process associated with the azimuthal distortion and bending of the vortex ring wherein ambient mass is brought in towards the jet-centreline along the major-axis side, and jet mass is ejected out along the minor-axis side. This non-uniform self-induction process results in enhanced mixing between the jet and the ambient irrotational mass<sup>(4-8)</sup>. As a result, the jet undergoes an axis-switching phenomenon wherein it entrains more fluid and spreads faster in the major-axis plane while it shrinks along the minor-axis side. The behaviour of coherent structures was also found to be strongly effected by initial flow conditions such as the jet aspect-ratio, initial momentum thickness, excited or unexcited and therefore could be manipulated<sup>(7)</sup>.

Means have also been explored to introduce secondary instabilities in the form of streamwise vortices generated from mixing devices such as tabs to alter the flow-field development significantly<sup>(12-20)</sup>. The mechanism of their formation, evolution, and interaction with Kelvin-Helmholtz type vortices is of great importance for practical applications. Generally tabs were observed to introduce circumferential variations in the jet flow development by splitting the jet into two high-velocity regions on either side of the diameter joining the two tabs<sup>(13)</sup>. Various tab configurations such as triangular and rectangular<sup>(16)</sup> have been studied in the past. The tab inclination<sup>(22)</sup>, with respect to the jet axis, has also been found to strongly govern the initial vortex-dynamics. Individual studies on the flow past a trapezoidal tab<sup>(23,24)</sup> mounted on a flat plate have also been carried out. However, the flow development downstream of a trapezoidal tab mounted on a flat plate (no-slip condition) changes significantly when such a tab configuration is in a jet flow (slip condition) at the nozzle exit. The focus of the present work was, therefore, to study the flow structure development behind a tab of trapezoidal configuration in a jet flow and its effect on the overall jet flow development, thereafter. Two such tabs are placed on the minor-axis sides (and tested for tab inclinations of 45° and 135° to the oncoming flow) of a 2:1 rectangular nozzle. Results are compared with the jet issuing from a 2:1 rectangular nozzle without tabs (hereafter referred to as the ‘plain jet’). A two-component hotwire probe (*X*-wire) was used for detailed grid measurements in the *Y*-*Z* plane of the jet in (i) the tab-wake region and, (ii) in the jet half-plane at various axial locations to study the flow structure development behind the tab and its effect on the overall jet flow development, respectively in the absence and presence of tabs.

## 2.0 EXPERIMENTAL SET UP AND PROCEDURE

### 2.1 Test facility and models

Experiments were carried out to investigate the jet flow development from a 2:1 rectangular nozzle, with and without tabs, Fig. 1(a). The nozzle has a circular section of  $203 \pm 0.1$  mm diameter, smoothly contoured to a rectangular section ( $2a = 47.0 \pm 0.1$  mm and  $2b = 23.5 \pm 0.1$  mm) over a length of  $300 \pm 0.1$  mm, where 2(a) and 2(b) are major- and minor-axis lengths, respectively. The equivalent diameter ( $D_e$ ) of the rectangular nozzle is  $37.5 \pm 0.1$  mm. The measurements are carried out at a nominal jet exit velocity ( $U_e$ ) of  $20 \pm 0.5$  ms<sup>-1</sup> and the Reynolds number based on the equivalent diameter of the jet ( $R_{De}$ ) is  $5.02 \pm 0.13 \times 10^4$ . A pair of trapezoidal tabs (2% total blockage) is placed in the minor-axis plane of a 2:1 rectangular nozzle to modify the initial jet development in this plane, Fig. 1(b).

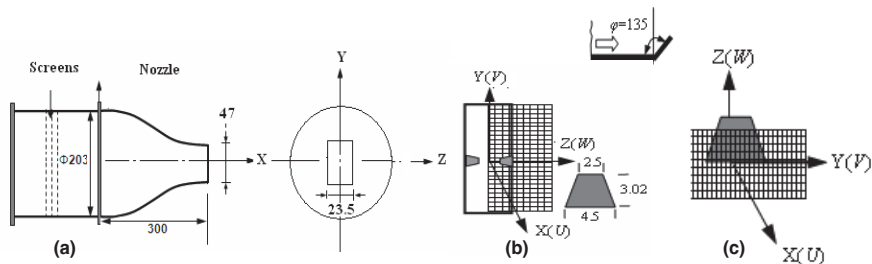


Figure 1. Schematic of (a) 2:1 rectangular nozzle, (b) tab placement ( $\phi=135^\circ$ ), tab dimensions and grid measurement plane for overall jet development study and, (c) near-wake grid measurement plane; all dimensions are in mm.

## 2.2 Instrumentation

Hot-wire measurements were carried out in the tab-wake region and at several axial locations in the  $Y$ - $Z$  plane by means of a 99N10 DANTEC anemometry system using a Dantec 55P11 2-component probe. The probe has platinum plated tungsten wires (1.25mm long and 5 $\mu$ m diameter) and can be used for air applications with turbulent intensities up to 5-10%. The  $X$ -wire was positioned in the flow in such a way that it allowed to measure the fluctuations of streamwise velocity ( $u'$ ) and transverse velocity ( $v'$ ). The positioning of the sensor was performed by using a PC controlled DANTEC 3-dimensional precision traverse (Model # 41T33). The probe was calibrated using Dantec 9054H01 calibrator with 120mm<sup>2</sup> nozzle in the velocity range between 0-25ms<sup>-1</sup>. The signals from the probe were acquired at a sampling rate of 3kHz with 10,000 samples. The anemometer analog output was acquired by using a differential mode National Instruments PCI -6036E having 16-Bit resolution, operating range of  $\pm 10$ V and maximum scan rate of 200Ks/samples. The linearisation and processing of the hot wire signal was then carried out digitally. The actual streamwise velocity  $U$  and perpendicular velocity  $V$  were calculated from the hotwire anemometer output according to King's law equation and equation procedure by Jorgenson<sup>(25)</sup>. The uncertainty in the jet exit velocity  $U_e$  and in the positioning of the hotwire  $X$ -probe is  $\pm 0.5$ ms<sup>-1</sup> (2.5%) and  $\pm 0.5$ mm (2%), respectively. The projected dimension of the sensor elements to the oncoming flow is 0.8mm and the uncertainty in measurements with regards to the probe dimensions is approximately 2%.

## 3.0 RESULTS AND DISCUSSIONS

### 3.1 Centreline velocity decay and jet half-width growth

In general, as the jet fluid moves away from its origin, it slows down due to the process of mixing initiated with slower moving ambient fluid. This interaction between the jet and the ambient fluid forms the mixing layer, or shear layer. Due to Kelvin-Helmholtz instability, the primary jet structures begin to roll-up which grow in size as they move downstream, due to entrainment of slower moving ambient fluid. As a result, jet decay is proportional to the velocity gradient across the shear layer and is a strong function of the distance downstream of the jet exit normalised by equivalent diameter of the nozzle. Figures 2(a) and (b) show the comparison of centreline velocity decay and their corresponding turbulent intensity plots, respectively. Relative to the plain jet, the potential core length of jets with tabs is significantly reduced from  $3.0D_e$

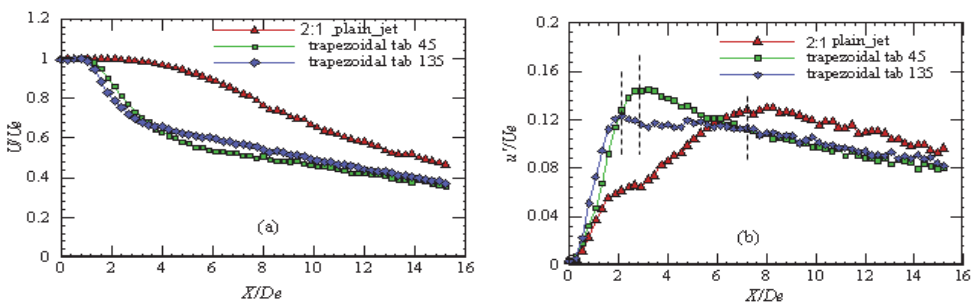


Figure 2. (a) Centreline velocity ( $U/U_e$ ) decay for jets issuing from a 2:1 rectangular nozzle with and without tabs and (b) effect of tabs on the  $u'/U_e$  centreline distribution.

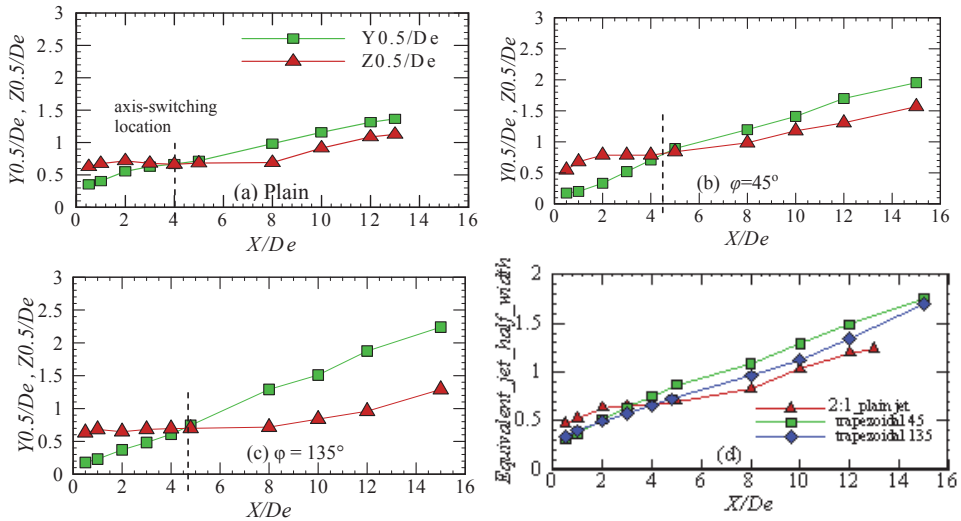


Figure 3. Half-width plots showing the variation in jet growth along Z- and Y-planes for the two tab inclination angles tested (a) plain jet, (b) jet with tab inclined at  $135^\circ$ , (c) jet with tab inclined at  $45^\circ$  and, (d) equivalent jet width for all the test cases.

to (for plain jet) to  $1.0D_e$  (by 67%) followed by a faster decay of the jet centreline velocity ( $U/U_e$ ), Fig. 2(a). For plain jet, the centreline turbulent intensity ( $u'/U_e$ ) shows a peak in value at  $X/D_e = 7.8$  whereas for jets with tabs this location shifts considerably upstream to  $X/D_e = 2.67$  for  $45^\circ$  tab followed by  $135^\circ$  tab at  $X/D_e = 2.0$ , Fig. 2(b). The above trends show enhancement of both large-scale and small-scale activity for jets with tabs relative to the plain jet and also with variation in tab inclination.

Figure 3 shows a comparison of the jet half-width growth for the test cases investigated. It can be seen and is well known, the plain jet from rectangular nozzle grows along its minor-axis plane while it shrinks along the major-axis plane. At approximately  $X/D_e = 4.0$ , the jet half-width plots along the two planes cross each other indicating the axis-switching location of the jet, Fig. 3(a). Tabs are initially seen to inhibit the jet growth along the minor-axis plane due to the blockage effect of the tabs. Thereafter for  $X/D_e > 4.0$ , the jet growth increases significantly. While the plain jet is observed to switch its axis at  $4.0D_e$ , the jet with tabs switch their axis at  $4.2\text{--}4.5D_e$ , Fig. 3(b)–(c). Further it can be observed that when the tab is inclined at  $45^\circ$  to the oncoming flow, the jet half-width growth increases significantly along the major-axis side but for the  $135^\circ$  inclined tab, the jet half-width growth increases significantly along the minor-axis side. This behaviour in jet growth is contrary to the results observed for cylindrical tabs<sup>(26)</sup> (placed  $90^\circ$  to the oncoming flow) in an elliptic jet where axis-switching did not occur due to reduced jet growth along minor-axis and enhanced jet growth along major-axis plane. This variation in the behaviour of jet growth with tab inclination angle becomes clear when the flow development in the tab wake region is discussed in detail in the later sections. The equivalent jet spread which signifies the overall mixing and jet spread along the axial location for a given exit condition is shown in Fig. 3(d). It can be seen that the overall jet growth is more for the jet with tabs and shows higher overall jet growth for tabs inclined at  $45^\circ$  followed by the jet with tabs inclined at  $135^\circ$ .

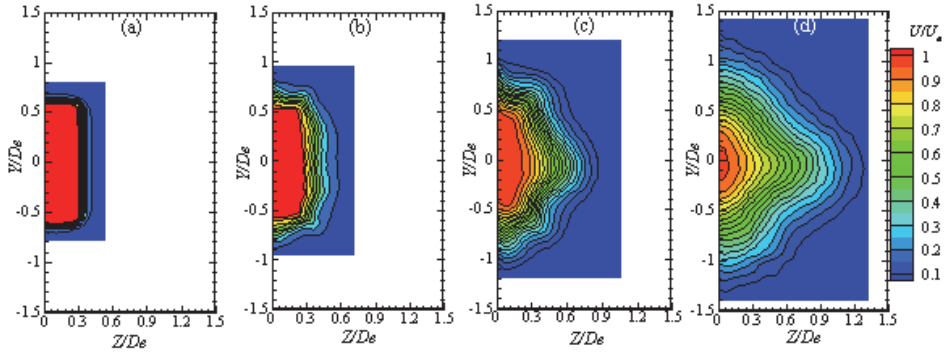


Figure 4. Contours of mean velocity at different axial locations in Y-Z plane for a plain jet a)  $X/D_e = 0.5$ , (b)  $X/D_e = 1.0$ , (c)  $X/D_e = 2.0$  (d)  $X/D_e = 4.0$ .

### 3.2 Overall jet development mean velocity distribution contours

Grid measurements were carried out at various axial locations to study the process of overall jet development. Extensive grid measurements were made in one-half Y-Z plane of the jet, Fig. 1 (b), with a step size of  $\Delta y = \Delta z = 1.0 \pm 0.1 \text{ mm}$  or  $0.026D_e$  for  $X/D_e = 0.5, 2.0$  (approx. 1,600 and 2,400 points, respectively) while a step size of  $\Delta y = \Delta z = 1.5 \pm 0.1 \text{ mm}$  or  $0.039D_e$  was kept for  $X/D_e = 3.0, 5$  (approx. 1,250 and 1,600 points, respectively). The variation in each successive contour level is  $0.1U_e$ . Contours of the normalised streamwise mean velocity ( $U/U_e$ ) in the tab wake region were also acquired at two streamwise locations  $X/w = 3.0$  and  $4.0$  (where  $w = 4.5 \text{ mm}$ ), respectively. These contours are obtained from grid measurements on both sides of the tab in the Y-Z plane (with  $\Delta y = \Delta z = 0.5 \pm 0.1 \text{ mm}$  or  $0.013D_e$  and resulting in 1,073 points), as shown in Fig. 1(c). Such detailed measurement grids were required because of the highly three-dimensional evolution of the flow behind the tab. The jet-exit shear-layer thickness ( $U = 0.99U_e$ ) along the minor-axis side,  $\delta_{mi}$ , was about 1.25mm at the tab axis and that along the major-axis side of the nozzle,  $\delta_{mj}$ , was 1.75mm, respectively. The corresponding displacement thickness along each nozzle axis is 0.381mm and 0.534mm, respectively. With respect to  $\delta_{mi}$  the tabs protrude well into the mean flow. The longitudinal turbulent intensity ( $u'/U_e$ ) at the jet exit was about 0.3% at  $20 \text{ ms}^{-1}$ . Figures 4, 5 and 7 show contours of normalised streamwise mean velocity ( $U/U_e$ ) for

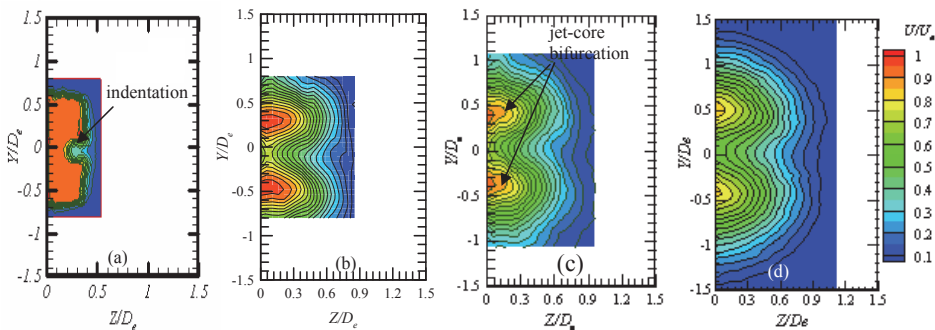


Figure 5. Contours of mean velocity at different axial locations in Y-Z plane for a trapezoidal tab with inclination of  $135^\circ$ . (a)  $X/D_e = 0.5$ , (b)  $X/D_e = 2.0$ , (c)  $X/D_e = 3.0$  (d)  $X/D_e = 5$ .

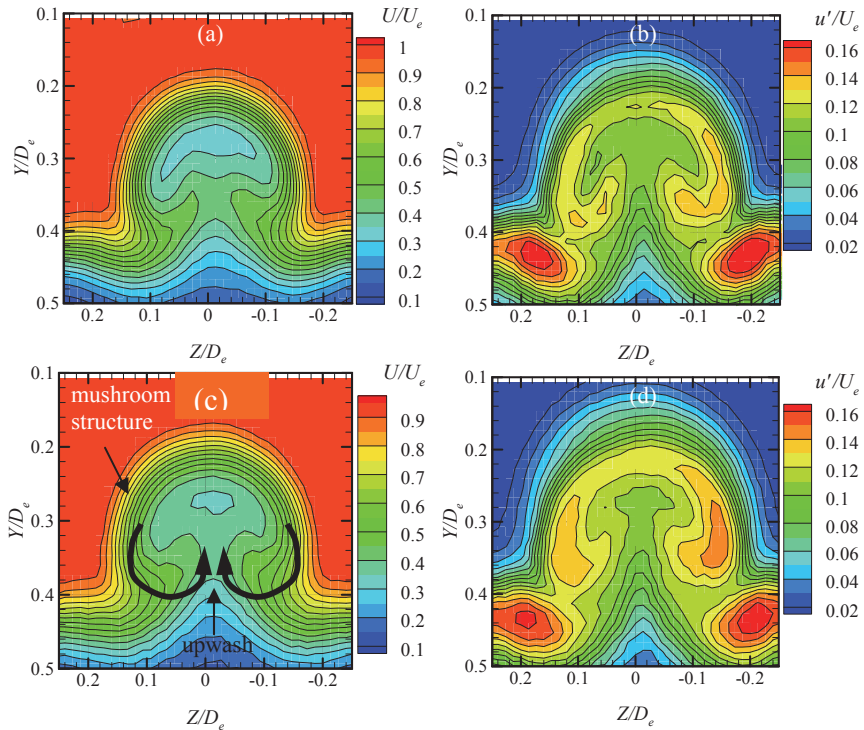


Figure 6. Contours of mean velocity and streamwise turbulence behind the tab at different axial locations in  $Y$ - $Z$  plane for tab inclination of  $135^\circ$ . (a)-(b)  $X/w = 3.0$  and, (c)-(d)  $X/w = 4.0$

each test case while Figs 6 and 8 show the flow development in the region of the tab-wake for various axial locations in the  $Y$ - $Z$  plane.

### 3.2.1 Plain jet

Immediately downstream of the nozzle exit, the plain jet is seen to retain its original rectangular shape and shows a thin mixing-layer initially<sup>(27)</sup>, as is evident from the closely spaced contours, Fig. 4(a). As the mixing between the jet and the ambient mass is initiated and the shear-layer grows, the jet begins to gradually deform due to non-uniform induction of velocity<sup>(4-8)</sup> along the nozzle azimuth, while vortices are generated from the nozzle corners (seen as a outward bump in contours), Fig. 4(b). Further downstream, the mixing layer begins to thicken and the jet cross section begins to change its shape as is indicated by a higher growth along minor-axis side (Fig. 4(a) – 4(d)). The spacing between the contour levels is seen to increase with increase in downstream distance. As a result, the jet undergoes a three-dimensional deformation process associated with the azimuthal distortion and bending of the rectangular vortex ring wherein ambient mass is brought in towards the jet centreline along the major-axis side, and jet mass is pushed out along the minor-axis side<sup>(7)</sup>.

### 3.2.2 Jet with tabs

Introduction of tabs in minor-axis side significantly modifies the local as well as the overall jet development, Fig 5 and 6. Tabs are seen to cause an inward indentation in the jet flow development due to the blockage effect that prevents the jet flow from reaching the tab-wake region immediately.

Such indentations help increase the contact area of the mixing layer with the slower moving ambient fluid resulting in enhanced mixing relative to the plain jet. However, the inward penetration of the tab wake initially inhibits the jet growth along the minor-axis side, as was observed for cylindrical tabs<sup>(26)</sup>. In fact, in the present tests, tabs not only bifurcate the jet core at some downstream distance but are also observed to enhance the jet growth along both planes, Fig. 3(b)–(c). This flow modification delays the overall axis-switching phenomena for both tab inclinations.

Variations in the overall jet flow development for the two tab inclinations tested can also be observed. The jet is observed to get bifurcated much earlier for tab inclination of  $135^\circ$  than for tab inclination of  $45^\circ$ . This modifies the jet development along each axis as observed in the jet half-width plots. Further details of the flow physics involved with tab inclination angle is studied using very fine grid measurements in the tab-wake region.

For tab inclination of  $135^\circ$ , the flow immediately behind the tab develops into a very well defined ‘mushroom structure’, Fig. 6(a) and (c). The mean velocity is seen to decrease sharply as the tab-wake region is approached, decreasing to approximately  $0.3U_e$  indicating strong cross-stream gradients. In the region of the tab-base, a sharp incursion of contours can be seen on each side of the tab which indicates the presence of a streamwise vortex (of clockwise rotation on right side and vice-versa). Such streamwise vortices are known to induce intense local mixing thereby promoting fluid and momentum exchange<sup>(26)</sup>. Further downstream the thickness of the mixing layer increases both along the tab axis and along the axis normal to the tab which results in the mushroom structure to grow in size. Figure 6(b) and (d) show the corresponding distribution of turbulence intensity in the tab wake region. It can be seen that the turbulence intensity is the highest on both sides of the tab base region and in the region of the streamwise vortices. The pair of streamwise vortices shed from each tab interacts with the azimuthal vortices embedded in the mixing layer and increase the entrainment of the mixing layer with the ambient fluid. The vortex system so generated is seen to split the jet-core at some downstream distance with high-velocity cores on either side of the minor-axis plane, Fig. 5(b)–(d). The observed jet bifurcation explains the significant reduction in jet core-length and the rapid centreline velocity decay associated with increased turbulent mixing activity thereafter for jets with tabs, as observed in Fig. 2.

Figure 7 shows contours of normalised streamwise mean velocity ( $U/U_e$ ) for a trapezoidal tab inclination of  $45^\circ$ . Some similar modifications in the overall jet flow development phenomena are observed in Fig. 6(a). However, the most notable feature is the much sharper inward indentation caused by this tab inclination, Figs 6(a) and 7(a). It can be seen that the flow while passing around

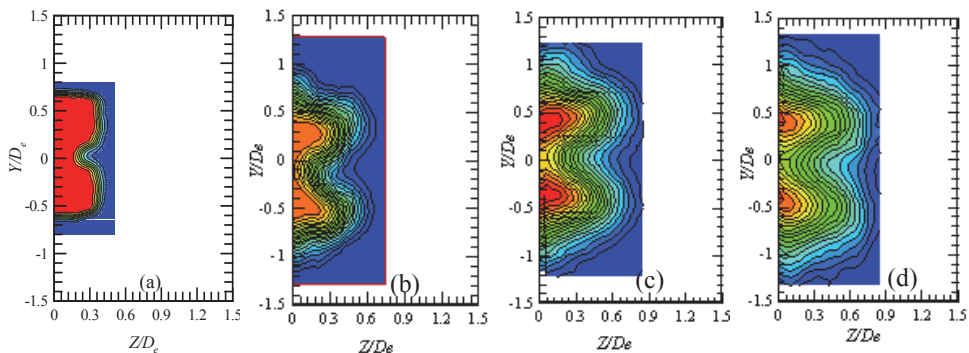


Figure 7. Contours of mean velocity at different axial locations in  $Y$ - $Z$  plane for a trapezoidal tab with inclination of  $45^\circ$ . (a)  $X/D_e = 0.5$ , (b)  $X/D_e = 2.0$ , (c)  $X/D_e = 3.0$  (d)  $X/D_e = 5$ .



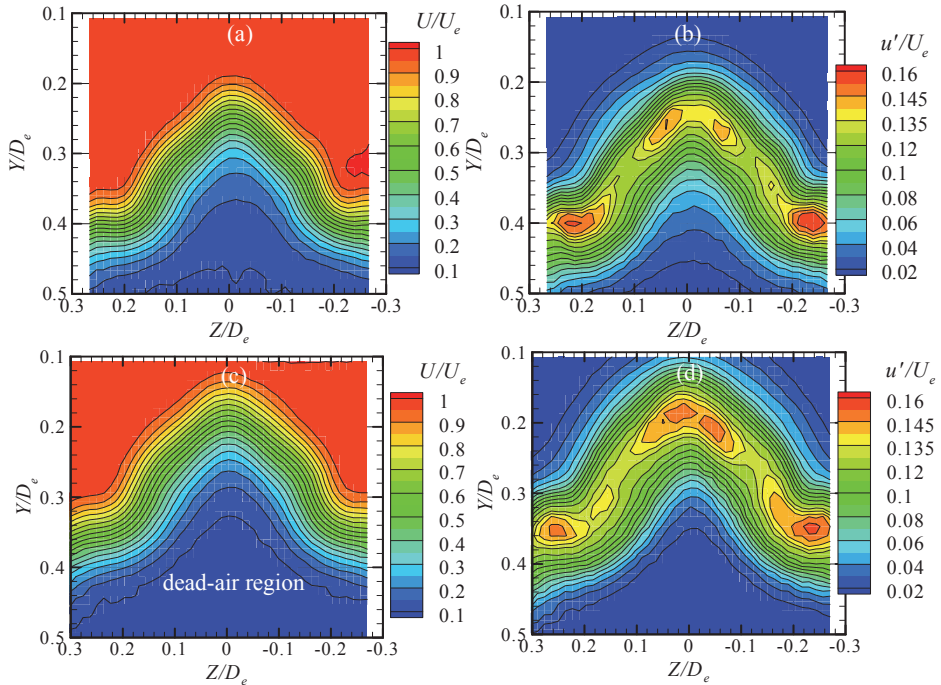


Figure 8. Contours of mean velocity and streamwise turbulence behind the tab at different axial locations in Y-Z plane for trapezoidal tab with inclination of  $45^\circ$ . (a)-(b)  $X/w = 2.0$  and, (c)-(d)  $X/w = 3.0$ .

the tab is unable to immediately reach behind the tab resulting in a huge portion of low speed or a dead air region, Fig. 8(a) and (c). Such a flow constraint imposed by this tab inclination prevents the flow behind the tab to develop into a mushroom structure as observed for  $135^\circ$  inclined tab. Instead the flow in the tab wake region takes the shape that resembles the tab configuration and with relatively more inward penetration, Fig. 6(c) and 8 (c). This change in flow development relatively inhibits the jet growth in the minor-axis plane while an increase in the jet growth along the minor-axis side is observed, Fig. 3(b) and (c). Figures 8(b) and (d) show the corresponding distribution of turbulence intensity in the tab wake region. It can be seen that the turbulence intensity is the highest at the top edges of the tab and in the region of the tab base. These variations suggest significant changes in flow structure development for tabs with different inclination angles to the oncoming flow.

### 3.2.3 Profiles of mean velocity and turbulence intensity

#### Along tab axis

Figures 9(a)-(c) show the mean velocity ( $U/U_e$ ) and turbulence intensity ( $u'/U_e$ ) profiles measured at various streamwise locations along the tab-axis ( $Z = 0$ ), respectively. For tab inclined at  $135^\circ$ , the mean velocity profiles reveal two distinct regions of velocity minimum and maximum, as seen in Fig. 9(a). Close to the base region of the tab (i.e., at  $Y/D_e = 0.32$ ) a maxima in  $U/U_e$  occurs (due to the upwash from the base vortex) that is followed by a velocity deficit or a minima between the tab mid-height and free-end (due to the downwash from the tab free-end). As the top-edge of the tab is approached, the  $U/U_e$  value is seen to increase to its value in the jet-core causing

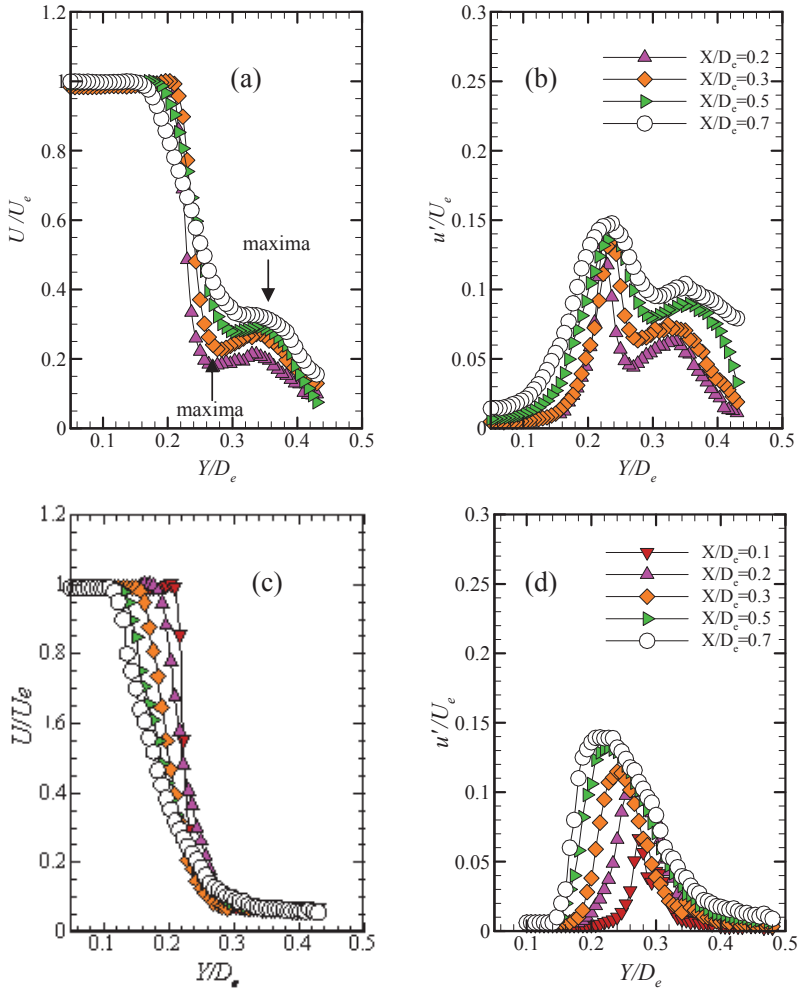


Figure 9. Profiles of mean velocity and turbulence intensity in the tab wake region with measurement plane parallel to the tab axis for (a)-(b)  $\phi = 135^\circ$  and (c)-(d)  $\phi = 45^\circ$ , respectively.

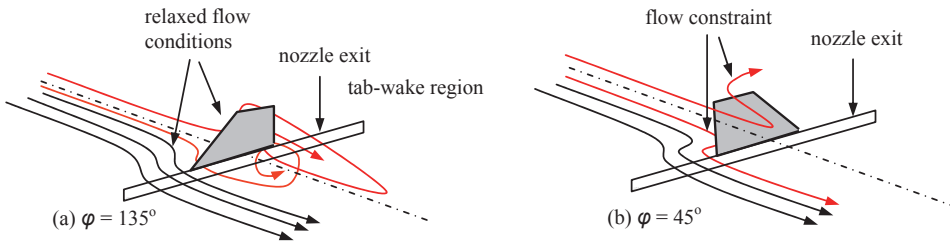


Figure 10. Schematic of the flow development from a tab at different inclination angles to the oncoming flow.

a shear layer to develop that gradually begins to roll-up into small-scale **K-H** vortices<sup>(26)</sup>. The corresponding turbulent intensity ( $u'/U_e$ ) profiles, Fig. 9(b), show intense local mixing in the region of the tab-base and the top edge of the tab. Further downstream, the velocity deficit at tab mid-span reduces (due to vortex interaction and viscous diffusion) and is seen to gradually move outwards while the shear layer from the tab top edge moves gradually inwards, between  $X/D_e = 0.5$  to  $0.7$ . On the other hand, for tab inclined at  $45^\circ$ , the mean velocity profiles do not show the presence of a velocity maximum and velocity minima in the region behind the tab, Fig. 9(c), as was seen in Fig. 9(a). This indicates that the tab inclination of  $45^\circ$  imposes a significant constraint on the oncoming jet flow so that the flow is unable to completely wrap around the tab and reach immediately behind it as seen for  $135^\circ$  inclined tab and also seen in Figs 6 and 8. The corresponding turbulence intensity plots also show a similar effect, Fig. 9(d).

Figure 10 shows a schematic of the flow development from each tab inclination developed based on the present results. It can be seen that as the flow approaches the tab, it has to move out of the way from the sides and over the top of the tab. For  $135^\circ$  tab inclination, the flow while passing over the tab is more 'relieved' in comparison with the flow passing over a  $45^\circ$  inclined tab, which is more constrained, Fig. 10(a) and (b). The flow before passing over the top of a  $45^\circ$  inclined tab first stagnates at the base of the tab and then speeds up over the top and sides to get out of the way of the tab causing larger changes in velocity, Fig. 10(b). On the other hand, for  $135^\circ$  tab inclination, the streamwise inclination eases the constraint on the flow (due to absence of flow stagnation) and so the flow freely moves over the top and sides in a more relaxed fashion resulting in lesser changes in velocity and pressure<sup>(28)</sup>, Fig. 10(a). These changes experienced by the flow due to variation in tab inclination result in different flow structure development in the wake of each tab inclination tested, as seen in Figs 6 and 8. From application point of view, it is preferable therefore to use a tab with  $135^\circ$  inclination because of its advantage of (i) lesser aerodynamic drag (due to significantly less constraint on the flow) and, (ii) less heat transfer, especially at the base of the tab in hot flows.

## 4.0 CONCLUSIONS

An experimental investigation was carried out to study the flow development of a jet issuing from a 2:1 rectangular nozzle, with a pair of trapezoidal tabs placed on its minor-axis side. Further, the effect of tab inclination ( $135^\circ$  and  $45^\circ$  to the oncoming flow) was also examined. Detailed two-component hotwire measurements were carried out to study the jet flow development.

Relative to the plain jet, the potential-core length of jets with tabs is significantly reduced (by 67%) followed by a faster decay of the centreline mean velocity ( $U/U_e$ ). This is accompanied by a significant upstream shift in the peak in centreline turbulence intensity ( $U'/U_e$ ). The above trends show enhancement of both large-scale and small-scale activity in jets with tabs. Close to the base of the tab ( $135^\circ$ ), a maxima in  $U/U_e$  occurs (due to the upwash from the base vortex) that is followed by a velocity deficit or a minima between the tab mid-height and free-end (due to the downwash from the tab free-end). Detailed grid study of the tab wake region shows that the flow immediately behind this tab develops into a very well defined mushroom structure with sharp incursion of contours on each side of the tab indicating the presence of a streamwise vortex that entrains the high-speed fluid from the jet-core towards the tab base and inwards along the tab axis resulting in a strong upwash. On the other hand with  $45^\circ$  tab inclination, the flow on passing around the tab is unable to immediately reach behind the tab resulting in a large portion of dead-air region near the tab base. Such a flow constraint imposed by this tab inclination prevents the flow behind the

tab to develop into a mushroom structure and takes a shape that resembles the tab configuration itself. However, the flow structure generated by the tabs (irrespective of its angle of inclination) is seen to split the jet-core at some downstream distance with high-velocity cores on either side of the minor-axis plane. The jet growth in each case is significantly enhanced both along minor-and major-axis planes which slightly delays the axis-switching location, relative to plain jet.

The results indicate that for  $135^\circ$  tab inclination (i.e., tab inclined in the direction the flow), the flow while passing over the tab is more relaxed in comparison with the flow passing over a  $45^\circ$  inclined tab (i.e., tab inclined against the flow), which is more constrained and results in different flow structure development in the wake of each tab. Since both tabs result in more or less similar enhanced mixing, from application point of view it would be preferable to use a tab with  $135^\circ$  inclination because of its potential from the view of improved jet mixing.

## ACKNOWLEDGEMENTS

The technical work reported here is carried out in the experimental Aerodynamics Division (EAD) at National Aerospace laboratories (CSIR), Bangalore. The first author is thankful to Dr A.R. Upadhy, Director NAL and Dr. Sajeer Ahmed, former Head EAD, for granting permission to carry out the experiments as a part of his PhD work. The authors also express their sincere thanks to Mr Sudhakar and Mr Manisankar (scientists, EAD) for their assistance in conducting the experiments.

## REFERENCES

1. GUTMARK, E., SCHADOW, K.C., KOSHIGOE, S. and WILSON, K.J. Combustion related shear flow dynamics in elliptic jets, *AIAA J*, 1989, **27**, (10), pp 1347-1353.
2. GUTMARK, E., SCHADOW, K.C. and WILSON, K.J. Subsonic and supersonic combustion related non-circular injectors, *J Propulsion and Power*, 1991, **7**, (2), pp 240-249.
3. QUINN, W.R. Experimental and numerical study of a turbulent free square jet, *Physics of Fluids*, 1988, **31**, (5), pp 1017-1025.
4. KROTHAPALLI, A., BAGDANOFF, D. and KARAMCHETI, K. On the mixing of a rectangular jet, *J Fluid Mechanics*, 1981, (107), pp 201-220.
5. MARSTERS, G.F. Spanwise velocity distributions in jets from rectangular slots, *AIAA J*, 1981, **19**, (2), pp 148-152.
6. HO, C.M. and GUTMARK, E. Vortex Induction and mass entrainment in a small-aspect-ratio jet, *J Fluid Mechanics*, 1987, (179), pp 383-405.
7. HUSSAIN, F. and HUSAIN, H.S. Elliptic jets, Part 1: Characteristic of unexcited and excited jets, *J Fluid Mechanics*, 1989, (208), pp 257-320.
8. QUINN, W. R. On mixing in an elliptic turbulent free Jet, *Physics of Fluids*, 1989, **1**, (10), pp 1716-1722.
9. VERMA, S.B. and RATHAKRISHNAN, E. Flow and acoustic properties of underexpanded elliptic-slot jets, **17**, (1), *AIAA J Propulsion and Power*, January – February 2001.
10. CRIGHTON, D.G. Instability of an elliptic jet, *J Fluid Mechanics*, 1973, **59**, pp 665-672.
11. GUTMARK, E.J. and GRINSTEIN, F.F. Flow control with non-circular jets, *Annual Review of Fluid Mechanics*, 1999, **31**, pp 239-272.
12. AHUJA, K.K. and BROWN, W.H. Shear Flow Control by Mechanical Tabs, AIAA paper 89-0094.
13. BRADBURY, L.J.S. and KHADEM, A.H. The distortion of a jet by tabs, *J Fluid Mechanics*, 1975, **70**, pp 801-813.
14. ZAMAN K.B.M.Q. Axis switching and spreading of an asymmetric jet: The role of coherent structure dynamics, *J Fluid Mechanics*, 1996, (316), pp 1-27.
15. CHUA, L.P., YU, S.C.M. and WANG, X.K. Flow visualization and measurements of a square jet with mixing tabs, *Experimental Thermal and Fluid Sciences*, 2003, **27**, pp 731-744.
16. VERMA, S.B., VENKATKRISHNAN, L. and RAMESH, G. 2-D PIV Study of Near-Field Flow Development from a 2:1 Elliptic Jet with Tabs AIAA Paper No-2007-4498.

17. TANNA, H.K. An experimental study of jet noise, part ii: shock associated noise, *J Sound and Vibration*, 1977, (50), pp 429-444.
18. NORUM, T.D. and SEINER, J.M. Broadband shock associated noise from supersonic jets, *AIAA J*, 1982, **20**, (1), pp 68-73.
19. KROTHAPALLI, A., WISHART, D.P. and MUNGAL, M.G. Supersonic jet control via point disturbances inside the nozzle, *AIAA J*, 1993, **31**, (7), pp 1340-1341.
20. ZAMAN K.B.M.Q., REEDER, M.F. and SAMIMY, M. Control of an axisymmetric jet using vortex Generators, *Physics of Fluids*, 1994, **6**, (2), pp 778-793.
21. BEHROUZI, P. and MCGUIRK, J.J. Effect of tab parameters on near-field jet plume development, *AIAA J Propulsion and Power*, 2006, **22**, (3), pp 576-585.
22. REEDER, M.F. and SAMIMY, M. The evolution of a jet with vortex real-time visualization and quantitative measurements, *J Fluid Mechanics*, 1996, **311**, pp 73-118.
23. GRETTA, W.J. and SMITH, C.R. The flow structure and statistics of a passive mixing tab, *J Fluids Engineering*, June 1993, **115**, pp 255-263.
24. DONG, S. and MENG, H. Flow past a trapezoidal tab, *J Fluid Mechanics*, 2004, **510**, pp 219-242.
25. JORGENSEN, F.E. Directional sensitivity of wire and fibre-film probes, *DISA Inf*, 1971, **11**, pp 31-37.
26. VERMA, S.B., SUDHAKAR, S. and VENKATKRISHNAN, L. Studies on an elliptic jet with cylindrical tabs, *J Turbulence*, 2010, **11**, (20), pp 1-24.
27. ARUN KUMAR, P., VERMA S.B. and ELANGO VAN. S. Study of jets from rectangular nozzles with square grooves, *Aeronaut J*, March 2011, **15**, (1165), pp 187-196.
28. *Fundamentals of Aerodynamics*, John Anderson, 4th ed, McGraw Hill, SIE, pp 474-475.